University of Pennsylvania
ScholarlyCommons

Departmental Papers (ESE)   Department of Electrical & Systems Engineering

1-2010

Super-High-Frequency Two-Port AlN Contour-Mode Resonators for RF Applications

Matteo Rinaldi
University of Pennsylvania, rinaldim@seas.upenn.edu

Chiara Zuniga
University of Pennsylvania, zunigac@seas.upenn.edu

Chengjie Zuo
University of Pennsylvania, chengjiezuo@hotmail.com

Gianluca Piazza
University of Pennsylvania, piazza@seas.upenn.edu

Follow this and additional works at: http://repository.upenn.edu/ese_papers

Part of the Acoustics, Dynamics, and Controls Commons, Electrical and Electronics Commons, Electro-Mechanical Systems Commons, Electronic Devices and Semiconductor Manufacturing Commons, Nanoscience and Nanotechnology Commons, Nanotechnology Fabrication Commons, Signal Processing Commons, and the Systems and Communications Commons

Super-High-Frequency Two-Port AlN Contour-Mode Resonators for RF Applications

Abstract

This paper reports on the design and experimental verification of a new class of thin-film (250 nm) superhigh-frequency laterally-vibrating piezoelectric microelectromechanical (MEMS) resonators suitable for the fabrication of narrow-band MEMS filters operating at frequencies above 3 GHz. The device dimensions have been opportunely scaled both in the lateral and vertical dimensions to excite a contourextensional mode of vibration in nanofeatures of an ultra-thin (250 nm) AlN film. In this first demonstration, 2-port resonators vibrating up to 4.5 GHz have been fabricated on the same die and attained electromechanical coupling, kt^2, in excess of 1.5%. These devices are employed to synthesize the highest frequency MEMS filter (3.7 GHz) based on AlN contour-mode resonator technology ever reported.

Disciplines

Acoustics, Dynamics, and Controls | Electrical and Computer Engineering | Electrical and Electronics | Electro-Mechanical Systems | Electronic Devices and Semiconductor Manufacturing | Nanoscience and Nanotechnology | Nanotechnology Fabrication | Signal Processing | Systems and Communications

Super-High-Frequency Two-Port AlN Contour-Mode Resonators for RF Applications

Matteo Rinaldi, *Student Member, IEEE*, Chiara Zuniga, *Student Member, IEEE*,
Chengjie Zuo, *Student Member, IEEE*, and Gianluca Piazza, *Member, IEEE*

Abstract—This paper reports on the design and experimental verification of a new class of thin-film (250 nm) super-high-frequency laterally-vibrating piezoelectric microelectromechanical (MEMS) resonators suitable for the fabrication of narrow-band MEMS filters operating at frequencies above 3 GHz. The device dimensions have been opportunely scaled both in the lateral and vertical dimensions to excite a contour-extensional mode of vibration in nanofeatures of an ultra-thin (250 nm) AlN film. In this first demonstration, 2-port resonators vibrating up to 4.5 GHz have been fabricated on the same die and attained electromechanical coupling, k_t^2, in excess of 1.5%. These devices are employed to synthesize the highest frequency MEMS filter (3.7 GHz) based on AlN contour-mode resonator technology ever reported.

I. Introduction

IN recent years, the use of micro- and nanoelectromechanical (MEMS/NEMS) resonators for RF applications has been widely explored. The development of compact, low cost, high-performance resonators is meant to respond to the growing demand of single-chip, multi-band RF solutions for advanced wireless communication systems. In addition, considering the rapid extension of wireless networks in the super-high-frequency (SHF) band, for example 3.6 GHz (802.11y) and 5 GHz (802.11a), the need for resonators operating in the SHF band is steadily growing. In this context, the scaling of MEMS/NEMS devices in the SHF band can have a tremendous impact because it will enable the fabrication of high-performance frequency control devices that, thanks to their compact form factor and IC integration capability, can be employed instead of cumbersome and unintegrable SAW devices, in next generation RF front-ends. In particular the fabrication of high-performance SHF channel-selector filters enables the implementation of receiver architectures capable of direct conversion at SHF with additional benefits in terms of complexity, cost, and power consumption.

Different MEMS resonator technologies based on electrostatic [1], [2] or piezoelectric [3], [4] transduction have been investigated. Among these, the AlN contour-mode

resonator (CMR) technology [3], [5] has emerged as one of the most promising solutions in enabling the fabrication of multiple frequency and high performance resonators on the same silicon chip. In fact, the CMR technology can combine in a single device many important features that characterize existing resonators (Fig. 1). The piezoelectric transduction enables simultaneous frequency scaling of the device and its direct interface to 50-Ω electronics. This is an extremely important advantage for RF applications (no matching networks with associated insertion losses are required) and it is not easily achievable with electrostatically-transduced resonators, for which frequency scaling is generally associated with an increase in the device impedance [6]. Even if an improved device impedance at higher frequency of operation was demonstrated using internal dielectric transduction [2], the values of the device impedance were still considerably high. In addition, the CMR technology has the same advantages of thin film bulk acoustic resonators (FBAR) over SAW devices in terms of miniaturization and IC integration capabilities. Filters exhibiting SHF and relatively large bandwidth (3%) utilizing FBARs have been demonstrated [7], [8]. In contrast to FBAR, the CMR technology enables the fabrication of multiple frequencies of operation on the same silicon chip. This feature is crucial for advanced wireless communication systems, for which single-chip, multi-band RF solutions are becoming the dominant trend.

High-performance AlN CMR devices in the very- and ultra-high-frequency (VHF-UHF) bands with quality factors between 1,000 and 4,000 have been previously demonstrated [5], [11]. Nevertheless, the capability of this technology to operate in the SHF band has not been extensively explored to date. Although one-port NEMS laterally-vibrating AlN resonators based on lateral field excitation (LFE) have been recently demonstrated by our group [12], the unconventional electrode configuration of those devices (bottom electrode not necessary for LFE) prevented the nanoresonators from being easily configured as 2-port networks, and hence fabrication of narrow-band filters. In this work, the thickness field excitation (TFE) CMR design is introduced to expand the frequency of operation of this technology in the SHF band to synthesize filters for emerging high-frequency wireless standards. The device dimensions have been scaled both in the lateral and vertical directions and a TFE scheme has been employed to excite a higher-order contour-extensional mode of vibration in nano-features of an ultra-thin (250 nm)
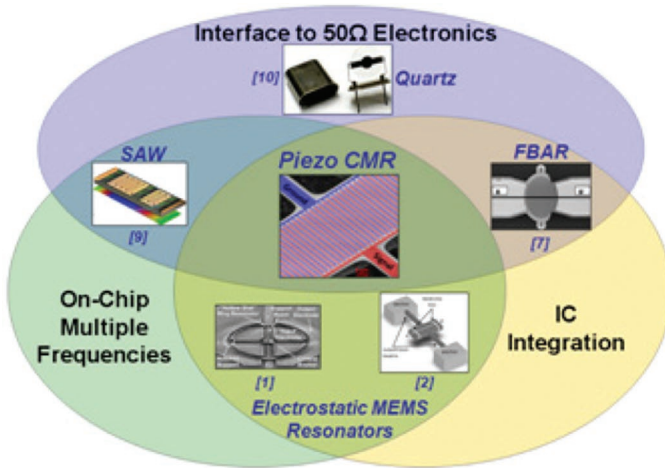
Fig. 1. Comparison diagram between contour-mode resonators (CMR) and other resonator technologies [1], [2], [7], [9], [10]. The diagram highlights the most important features of modern resonant devices for filtering applications.
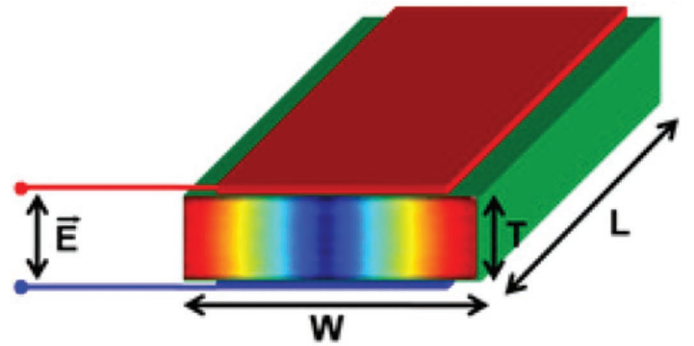

Fig. 2. Schematic representation of a contour-mode resonator with overlapped 2-D finite element modeling simulation of the device total displacement at resonance.

AlN film up to 4.5 GHz. A 2-port configuration has been implemented for the resonators presented here and the highest frequency (3.7 GHz) filter based on self-coupled AlN CMRs [11] was synthesized by simply electrically cascading 2 resonator stages.

II. DESIGN

A conventional CMR is composed of an AlN film sandwiched between 2 metal electrodes (Fig. 2). When an AC signal is applied across the thickness (T) of the device a contour-extensional mode of vibration is excited through the equivalent d_{31} piezoelectric coefficient of AlN. Given the equivalent mass density, ρ_{eq}, and Young's modulus, E_{eq}, of the material stack that forms the resonator, the center frequency, f_0, of this laterally vibrating mechanical structure, is set by the width, W, of the AlN plate and can be expressed as [13]:

$$ f_0 = \frac{1}{2W} \sqrt{\frac{E_{\mathrm{eq}}}{\rho_{\mathrm{eq}}}}. \tag{1} $$

The other 2 geometrical dimensions, length, L, and thickness, T, can be independently selected to set the resonator electrical capacitance, C_0, and its motional resistance, R_{m} [3], as:

$$ R_{\mathrm{m}} \propto \frac{T}{L} $$
$$ C_0 \propto \frac{LW}{T}. \tag{2} $$

To scale the resonance frequency, f_0, above 3 GHz (SHF band), the width, W, needs to be reduced below ~1.2 µm (the exact value depends upon E_{eq} and ρ_{eq} and therefore the thickness and material properties of the AlN/metal

stack). The reduction in width causes a considerable decrease in the device capacitance, C_0, to the point that its value can fall below the parasitic capacitance of the supporting substrate (silicon in this case). These parasitics negatively affect the electrical response of the device and can completely mask the device output signal. Therefore, scaling of the device resonance frequency into the SHF band is constrained by the need to keep the value of C_0 above the parasitic capacitances and simultaneously occupying a small form factor. Specific scaling rules as illustrated in the following section should therefore be followed.

A. Scaling Rules

To attain higher frequency of operation, W needs to be made smaller. At the same time, taking into account the constraints on C_0, the surface area of the CMR needs to be increased and its thickness reduced (2). For this purpose, the following criteria are proposed as guidelines for scaling the AlN CMR into the SHF range:

- Mechanically couple a large number, n, of sub-resonators whose width, W, has been scaled to operate in the SHF band [Fig. 3(b)]. In this way a higher-order mode of vibration is excited in the AlN plate (f_0 is set by W), but the capacitance of the device is n times larger (total width equal to $n \cdot W$).
- Reduce the thickness, T, of the AlN film [Fig. 3(c)]. This is extremely important to further increase the device capacitance while simultaneously keeping small the effective area occupied by the device.
- Reduce the length, L, of the resonator [Fig. 3(d)] to avoid loading the quality factor of the device with the electrical resistance of the metal electrodes. The reduction in the length of the electrode compensates for the increase in resistance associated with the scaling of the electrode width.

The devices presented in this work were designed in accordance to these design rules to operate at frequencies above 3 GHz. A 2-port configuration was chosen, because
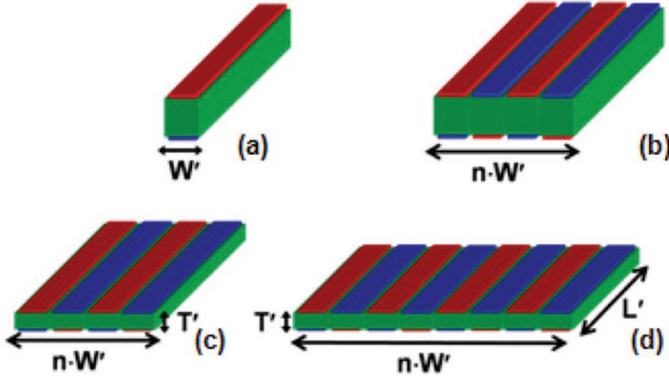
Fig. 3. Schematic representation of the contour-mode resonator scaling to super high frequency: (a) scaling of the width to increase the frequency, (b) mechanical coupling of a large number of scaled sub-resonators to increase the device capacitance, (c) reduction of the AlN film thickness to increase capacitance and reduce device form factor, (d) reduction of the device length to compensate for increase in electrode resistance caused by scaling of the width.

it enables the synthesis of narrow-band filters by simply electrically cascading 2 resonator stages.

B. SHF Two-Port AlN CMR Design

The SHF 2-port AlN CMR resonator (Fig. 4) of this work consists of an ultra-thin (250 nm) AlN film sandwiched between bottom Pt (50 nm) and top Au (100 nm) electrodes. The bottom Pt is a single electrode connected to electrical ground, and the top Au layer (chosen for its very low resistivity) is patterned in n parallel electrodes whose width varies between 0.4 and 0.7 μm depending upon the desired frequency of operation.

A number n_{in} of the top Au electrodes are connected to form the input port and the remaining (n_{out}) are used to form the output port. The frequency setting width, W, of the sub-resonators forming the electromechanical structure was varied between 0.7 and 1.2 μm to achieve resonance frequencies between 3 and 4.5 GHz. The number, n, of mechanically coupled sub-resonators was varied between 37 and 67 and the device length, L, was fixed to 17 μm.

The equivalent electrical model of the 2-port AlN CMR is shown in Fig. 5. All the equivalent electrical parameters can be expressed as a function of the resonator capacitance, C_o, the frequency of operation, ω_o, the electromechanical coupling, k_t^2, and quality factor, Q [14]. These relations are explicit expressed as

$$C_o = C_{0,\text{in}} + C_{0,\text{out}} = (n_{\text{in}} + n_{\text{out}})\varepsilon_0 \varepsilon_{33} \frac{WL}{T}$$

$$R_{\text{m}} = \frac{\pi^2}{2} \frac{1}{\omega_0 C_0 k_t^2 Q}; \quad C_{\text{m}} = \frac{2}{\pi^2} C_0 k_t^2 \quad (3)$$

$$L_{\text{m}} = \frac{\pi^2}{2} \frac{1}{\omega_0^2 C_0 k_t^2}; \quad \omega_0 = 2\pi f_0,$$

where ε_0 is the free space permittivity and ε_{33} the AlN permittivity. The device capacitance is modeled as a par-
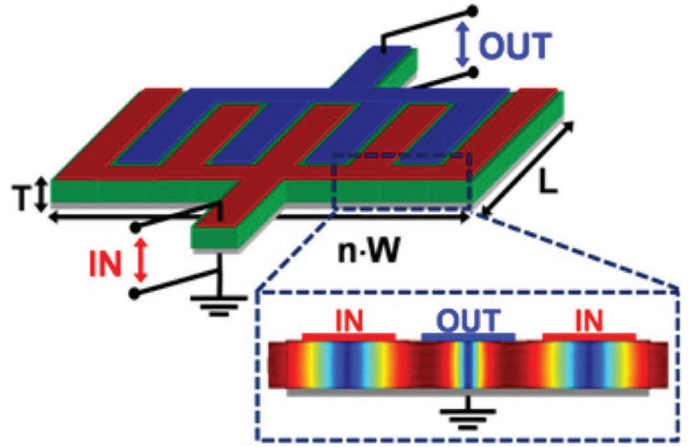

Fig. 4. Schematic representation of the designed super-high-frequency 2-port contour-mode resonator. The inset shows a finite element modeling simulation of the device 2-D total displacement: when an ac signal is applied to the input port, the electric field across the thickness of the AlN causes an in-plane deformation of the structure through the equivalent d_{31} piezoelectric coefficient and excites the resonator in a contour-extensional mode of vibration (it vibrates along its width, W). Because of the direct piezoelectric effect, charge is generated and collected by the sensing electrodes (output port).
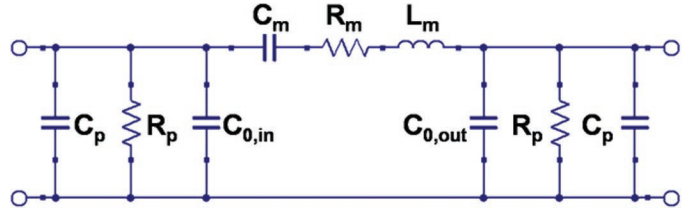

Fig. 5. Equivalent electrical circuit for the 2-port AlN contour-mode resonator. C_{p} and R_{p} are parasitic components due to the substrate.

allel plate capacitor and it does not take into account fringing field effects.

C. SHF Narrow-Band CMR Filter Design

The configuration of the CMR device as a 2-port network enabled the direct synthesis of the first prototype of SHF filters based on CMR technology. For this purpose, 2 resonator stages were electrically cascaded in series to form narrow band filters operating up to 3.7 GHz.

The coupling technique is based on the use of the intrinsic capacitance of a 2-port device and permits the definition of band pass filters by simply employing same frequency resonators [11]. This is different from conventional ladder configurations [15], which require 2 different frequency devices and have an associated negative impact on filter yields.

The equivalent electrical model of the second order filter based on self-coupled AlN CMRs is shown in Fig. 6.

According to (3), the electromechanical coupling, k_t^2, sets the value of the motional capacitance, C_{m}, given the geometrical capacitance, C_0, of the device. The parasitic capacitance in parallel with the input and output ports of the CMRs modify the ratio between motional and electri-
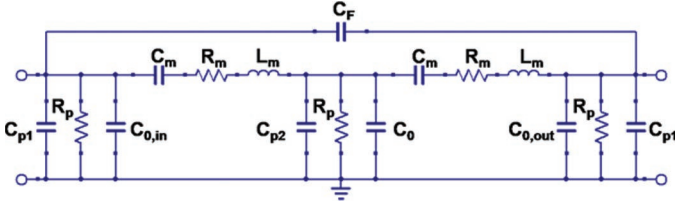
Fig. 6. Equivalent electrical circuit for the second order filter based on self-coupled AlN contour-mode resonators. C_{p1}, C_{p2}, R_p are the parasitic component in parallel with the input and output ports of the device; C_f is the parasitic feed-through capacitance between input and output ports.
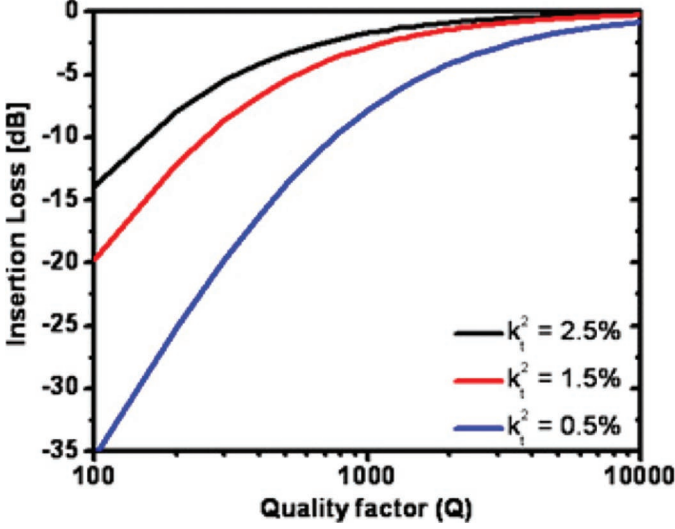

Fig. 7. Analytical simulation of the insertion loss of the second-order contour-mode resonator filter for different values of k_t^2 and Q.
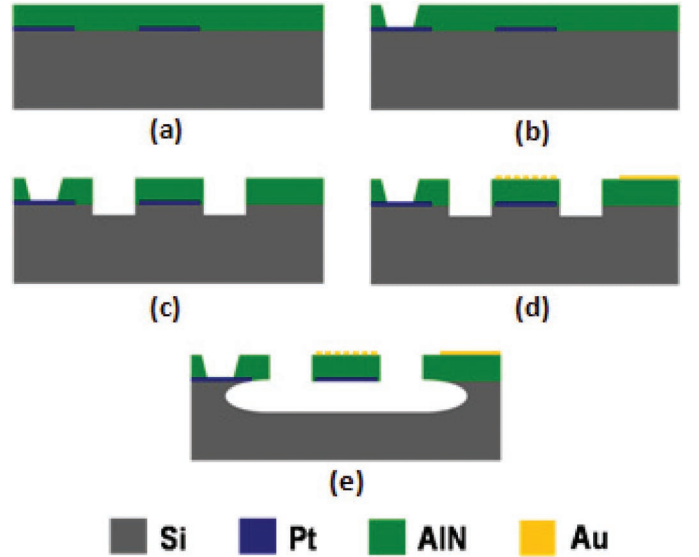

Fig. 8. Four-mask post-CMOS compatible fabrication process: (a) sputter-deposition of Pt and of the ultra-thin (250 nm) AlN film on high resistivity Si substrate, (b) open vias in AlN to access the bottom electrode, (c) dry etching of AlN in Cl$_2$ based chemestry, (d) patterning of the top Au electrode by electron-beam lithography and lift-off, (e) XeF$_2$ dry release of the AlN resonator.

cal capacitance of the resonators and reduces the effective electromechanical coupling of the system according to

$$k_{t,\text{eff}}^2 = \frac{\pi^2}{2} \frac{C_m}{C_0 + C_p}. \tag{4}$$

The decrease in the effective electromechanical coupling reduces the bandwidth of the filter accordingly:

$$\text{BW}_{3\text{dB}} \approx \sqrt{1 + \frac{2C_m}{C_0 + C_p}} - 1 \approx \frac{C_m}{C_0 + C_p} = \frac{2}{\pi^2} k_{t,\text{eff}}^2. \tag{5}$$

The insertion loss of the filter is also affected by the value of the effective electromechanical coupling. In fact, only the fraction of the input electrical signal that is not lost in the parasitic components is converted into mechanical vibration by the CMR transducer. This physical behavior is highlighted by the analytical simulation shown in Fig. 7, in which the insertion loss of the system is plotted as a function of k_t^2 and Q. As can be seen from the plot, the k_t^2 plays a significant role in setting the filter insertion loss.

These points further justify the need to maintain the value of the device capacitance, C_0, well above the parasit-

ics when scaling the device to higher frequencies of operation.

III. FABRICATION PROCESS

The devices presented in this work were fabricated combining optical and electron-beam lithography techniques. A 4-mask post-CMOS compatible fabrication process was employed (Fig. 8).

The platinum (Pt) bottom electrode was first patterned by lift-off on top of a high resistivity silicon wafer. The ultra-thin (250 nm) AlN film was sputtered deposited using a Tegal Endeavor tool (Tegal Corp., Petaluma, CA) and its quality was optimized to achieve rocking curve values as good as 2.1° (equivalent to what has been obtained in micron-size devices). The optimization was conducted in collaboration with Tegal Corporation. Vias to the bottom electrode pads were opened in the thin AlN film by wet etching in phosphoric acid (H$_3$PO$_4$). Optical lithography was performed for the definition of both the top electrode contact pads and the alignment marks for the subsequent electron-beam lithography step. The in-plane dimensions of the resonators were defined by dry etching of the ultra-thin AlN film in Cl$_2$-based chemistry using photoresist as a mask. The top gold electrode pattern was defined by electron-beam lithography and lift-off. The device was released from the silicon substrate by isotropic dry etching in XeF$_2$.

It is worth noting that, although electron-beam lithography was employed, the minimum lithographic features (400 nm) used to make these devices can also be defined
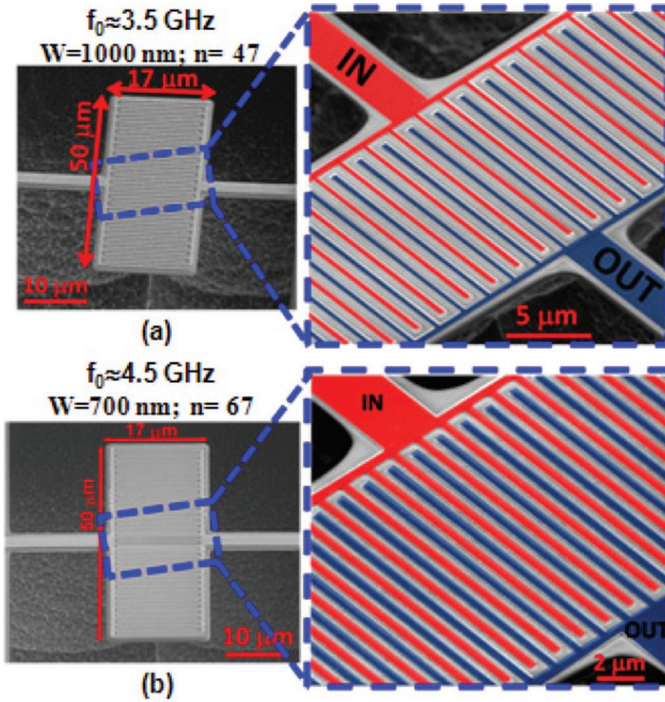
Fig. 9. Scanning electron micrographs of the fabricated 3.5-GHz (a) and 4.5-GHz (b) 2-port contour-mode resonators. The metallization ratio (ratio of metal electrode to AlN surface) is 50% for the 3.5-GHz device and 75% for the 4.5-GHz device.

by state-of-the-art optical lithography used in CMOS foundries.

The scanning electron micrographs of 2 of the fabricated devices are shown in Fig. 9. The highest frequency of operation, 4.5 GHz, is achieved by scaling the width of each sub-resonator to 700 nm.
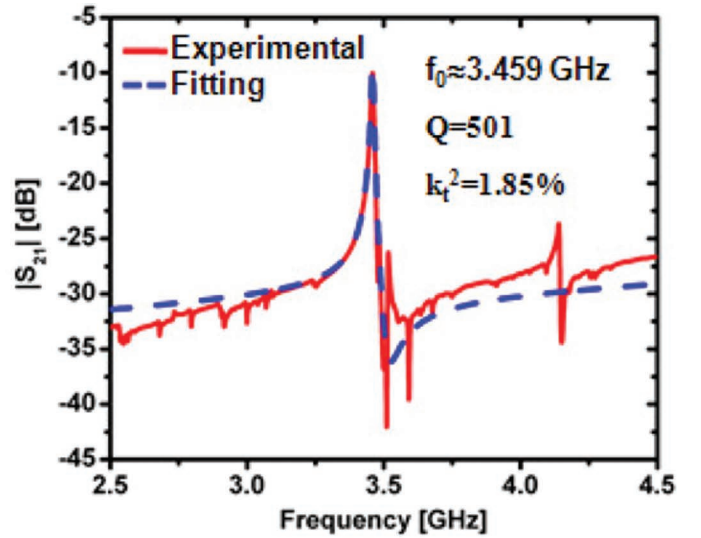
IV. EXPERIMENTAL RESULTS AND DISCUSSION

The fabricated devices were tested in an RF probe station and the scattering parameters were measured by an Agilent N5230A network analyzer (Agilent Technologies, Santa Clara, CA) after performing a short-open-load-through (SOLT) calibration on a reference substrate.
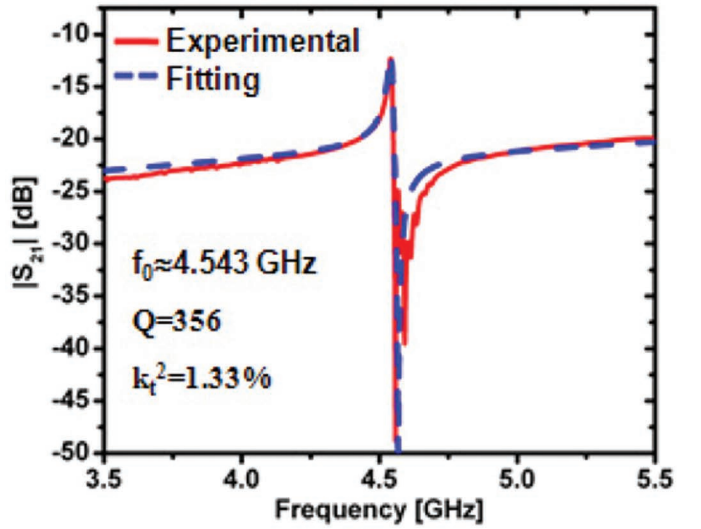
A. SHF 2-Port CMRs

The measured electrical responses of the SHF 2-port CMRs were fitted to the equivalent electrical circuit in Fig. 5 and both the experimental and fitted curves are shown in Fig. 10. The values of the parasitic components, C_p and R_p, were measured by means of de-embedding structures fabricated on the same silicon chip. The quality factor, Q, and the intrinsic electromechanical coupling, k_t^2, of the resonators were extracted according to (3).

It is important to note that an $f \cdot Q$ product as high as $1.7 \cdot 10^{12}$ Hz has been measured. This value is approximately one order of magnitude greater than the one measured for lower frequency 2-port CMRs [11]. Regard-

Fig. 10. Experimental response and equivalent model fitting of the fabricated 3.5-GHz (a) and 4.5-GHz (b) 2-port contour-mode resonators.

TABLE I. DIMENSIONS AND EXTRACTED PARAMETERS OF FABRICATED CONTOUR-MODE RESONATORS.

Frequency of operation [GHz]	k_t^2	Q	$n \cdot W$ [µm]	L [µm]
3.04	1.5%	520	37 × 1.2	17
3.46	1.85%	500	47 × 1	17
4.54	1.3%	360	67 × 0.7	17

ing the $k_t^2 \cdot Q$ product, a value as high as 9.3 has been measured. This is at least 5 times higher than the one reported by the same group for SHF lateral field excited (LFE) NEMS resonators [12]. The higher k_t^2 enables the synthesis of narrow-band SHF filters.

A list of the fabricated CMRs operating above 3 GHz along with the corresponding geometrical dimensions and values of k_t^2 and Q is reported in Table I.
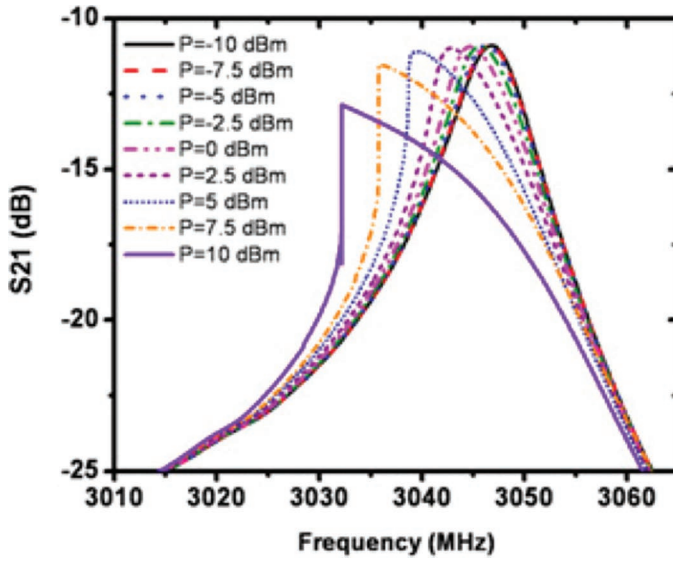
Fig. 11. Transmission responses for different input power level of the fabricated 3-GHz AlN contour-mode resonator. The presence of bifurcation is considered to be the point of maximum power handling for the resonator.

The power handling capability of the scaled CMRs was also experimentally analyzed. The response of a fabricated 3-GHz resonator was measured for different values of the input available power. The maximum value of available input power before bifurcation [16] occurs (Fig. 11) was estimated to be approximately 5 dBm. This experimental value of maximum usable power is comparable to the one reported for other devices only if opportunely scaled by the actual value of the device input impedance (if different from 50 Ω) and divided by the volume of the mechanical structure. By taking this into account, the current flowing into device at resonance (for 5 dBm available power at the input port) corresponds to a value of critical power density of approximately 5.96 μW/(μm^3). This value is at least 20 times higher than the one measured for low frequency CMRs, and shows another advantage of scaling the CMRs to super high frequencies.

The temperature coefficient of frequency (TCF) of the fabricated nano resonators was also measured and found to be -43.7 ppm/°C. This value is higher than what is encountered in equivalent MEMS devices [3]. This is due to the effect of the top gold electrodes, whose thickness (100 nm) becomes a considerable fraction of the AlN (250 nm) film in the NEMS implementation [12].

B. SHF Second-Order Filters Based on AlN CMRs

The measured electrical responses of the fabricated SHF narrow-band filters are shown in Fig. 12. The data was fitted to the equivalent electrical circuit shown in Fig. 6. The values of the parasitic components were measured by means of on-chip integrated de-embedding structures. Note that the filter response of Fig. 12 also includes the parasitics and no de-embedding was performed.
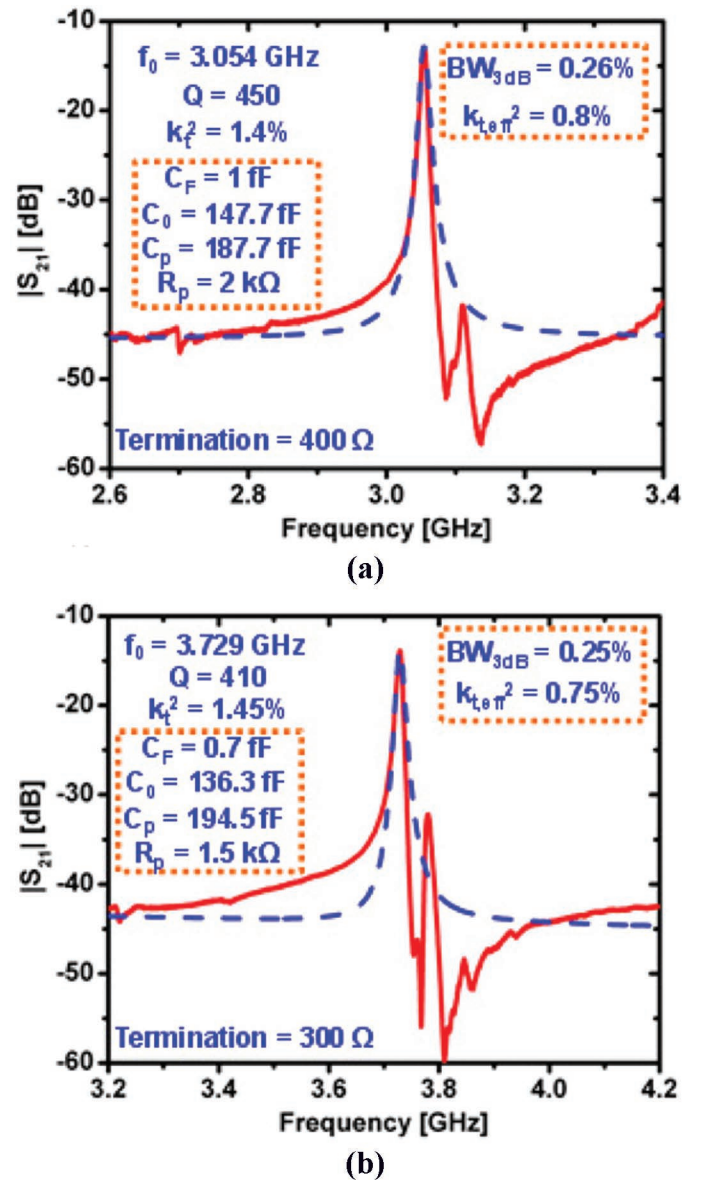

(a)

(b)

Fig. 12. Experimental response and equivalent model fitting of the fabricated 3-GHz (a) and 3.7-GHz (b) second-order filters based on 2 self-coupled contour-mode resonators. Q and k_t^2 values refer to the individual resonators forming the filter.

In these filters, the measured values of the device's geometrical capacitance and parasitics are comparable. This, as explained in Section II, greatly reduces the effective electrometrical coupling of the filters, therefore reducing the device's bandwidth and increasing its insertion loss. To simulate the de-embedded response of the filter, the measured parasitic capacitance, C_p, was removed from the equivalent circuit of the filter. In Fig. 13 the de-embedded response of the 3-GHz filter is plotted for different values of quality factor, Q, and compared with the one that includes parasitics. For the actual measured value of the resonator Q (450) an improvement in insertion loss of approximately 6 dB is observed for the de-embedded response. At the same time, if the parasitic effects were to be removed, the filter bandwidth would increase up to
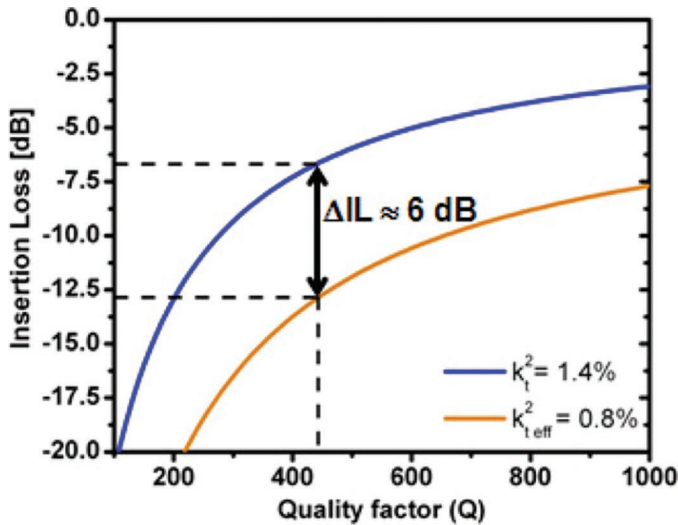
Fig. 13. De-embedded ($k_t^2 = 1.4\%$) and as-fabricated ($k_{t,\text{eff}}^2 = 0.8\%$) insertion loss of the 3-GHz filter plotted for different values of quality factor, Q.
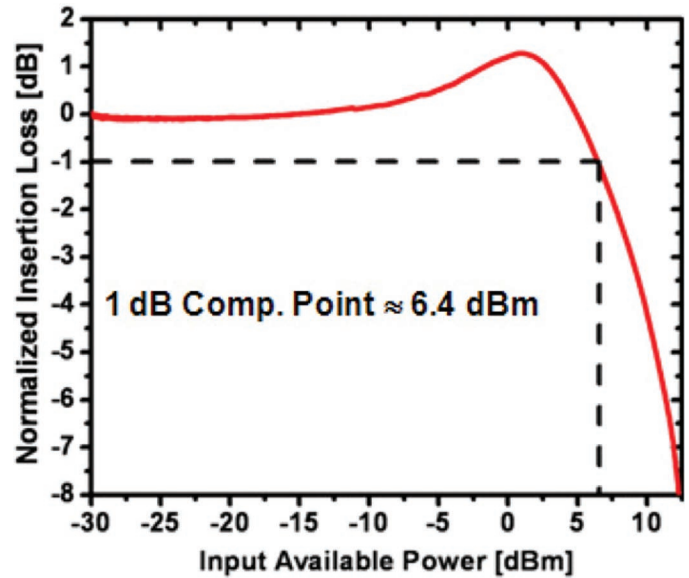

Fig. 14. Power handling measurement for the fabricated 3.7-GHz second-order contour-mode resonator filter. The improvement in insertion loss before the 1-dB compression is not yet understood.

the value set by the intrinsic electromechanical coupling of the fabricated CMRs according to (5). The improved value of insertion loss (~6.5 dB) and wider bandwidth could also be attained on the same silicon substrate by simply making the device capacitance, C_0, larger and well above the parasitic components. Additionally, the parasitics can be further reduced by optimizing the configuration of the test pads.

The power handling capability of the fabricated SHF filters was experimentally characterized by measuring their 1-dB compression point. A value of available power of 6.4 dBm was recorded for the 1-dB compression of the 3.7-GHz filter (Fig. 14).

For low frequency CMR filters, with a volume at least 100 times greater than the one of the SHF devices presented here, a 1-dB compression point of 10 dBm was measured [11]. This study shows that the SHF filters can ultimately handle more power per unit volume and, if appropriately sized, can withstand much higher power levels than the devices at lower frequencies. This is a clear evidence of the fact that the CMR technology can be advantageously scaled to higher frequencies.

These devices represent the first prototype of SHF filters based on AlN CMRs. The filters' performance can be improved to a large extent by optimizing the resonator in-plane geometry to increase the transducer capacitance and by acting on the figure of merit, $k_t^2 \cdot Q$, of the device.

V. CONCLUSION

In this paper, the design, fabrication, and testing of 2-port AlN CMRs operating in the SHF band up to 4.5 GHz was demonstrated. Design issues and scaling rules to operate AlN CMRs above 3 GHz were introduced and discussed. An ultra-thin (250 nm) AlN film was employed

to fabricate SHF resonators with values of electromechanical coupling, k_t^2, in excess of 1.5% and $f \cdot Q$ product as high as $1.7 \cdot 10^{12}$ Hz. The effect of frequency scaling on power handling was experimentally analyzed and a value of critical power density of approximately 5.96 $\mu W/(\mu m^3)$ was recorded for a fabricated 3-GHz CMR. This value shows that at least one order of magnitude improvement in power handling can be obtained by moving the CMR technology from megahertz to gigahertz frequencies. The capability of these devices to be employed for the fabrication of narrow-band filters was proven by synthesizing the highest frequency (3.7 GHz) 2nd-order filter based on electrically self-coupled AlN contour-mode devices. The importance of the $k_t^2 \cdot Q$ product on the filter performance (insertion loss and bandwidth) was analyzed and the effect of parasitic components on the response of the SHF filters was modeled. The demonstrated features and the disclosed potentialities of the SHF-scaled CMR technology suggest that it is an excellent candidate for the implementation of compact, low-power, high-performance RF components for radar communications and other SHF wireless applications.

REFERENCES

[1] C. T.-C. Nguyen, "MEMS technology for timing and frequency control," *IEEE Trans. Ultrason. Ferroelectr. Freq. Control*, vol. 54, no. 2, pp. 251–270, Feb. 2007.

[2] D. Weinstein and S. A. Bhave, "Internal dielectric transduction of a 4.5 GHz silicon bar resonator," in *IEEE Int. Electron Devices Meeting*, Dec. 2007, pp. 415–418.

[3] G. Piazza, P. J. Stephanou, and A. P. Pisano, "Piezoelectric aluminum nitride vibrating contour-mode MEMS resonators," *J. Microelectromech. Syst.*, vol. 15, no. 6, pp. 1406–1418, Dec. 2006.

[4] R. Abdolvand, G. K. Ho, J. Butler, and F. Ayazi, "ZnO-on-nanocrystalline-diamond lateral bulk acoustic resonators," in *Proc. 20th IEEE Int. Conf. Micro Electro Mechanical Systems*, Kobe, Japan, Jan. 2007, pp. 795–798.

[5] P. J. Stephanou, J. P. Black, and A. L. Benjamin, "Miniaturized multi-band filter banks for extravehicular radio (EVA) applications," in *Proc. IEEE Radio Frequency Integrated Circuits Symp.*, Atlanta, GA, Jun. 2008, pp. 171–174.

[6] D. L. DeVoe, "Piezoelectric thin film micromechanical beam resonators," *Sens. Actuators A*, vol. 88, pp. 263–272, 2001.

[7] M. Hara, T. Yokoyama, M. Ueda, and Y. Satoh, "X-Band filters utilizing AlN thin film bulk acoustic resonators," in *Proc. IEEE Ultrasonic Symp.*, New York, NY, Oct. 2007, pp. 1152–1155.

[8] K. M. Lakin, "Thin film resonators and filters," in *Proc. IEEE Ultrasonic Symp.*, Nevada, USA, Oct. 1999, vol. 2, pp. 895–906.

[9] Introduce to Saw filter. ITF, Bucheon, Korea. [Online] Available: http://www.itf.co.kr/tech/sub3.htm

[10] Fortiming Corporation, Marlborough, MA. [Online] Available: http://www.4timing.com/qcm.htm

[11] C. Zuo, N. Sinha, M. B. Pisani, C. R. Perez, R. Mahameed, and G. Piazza, "Channel-select RF MEMS filters based on self-coupled AlN contour-mode piezoelectric resonators," in *Proc. IEEE Ultrasonics Symp.*, New York, NY, Oct. 2007, pp. 1156–1159.

[12] M. Rinaldi, C. Zuniga, and G. Piazza, "5–10 GHz AlN contour-mode nanoelectromechanical resonators," in *22nd IEEE Int. Conf. Micro Electro Mechanical Systems*, Sorrento, Italy, Jan. 2009, pp. 916–919.

[13] P. J. Stephanou, G. Piazza, C. D. White, M. B. J. Wijesundara, and A. P. Pisano, "Piezoelectric thin film AlN annular dual contour mode bandpass filter," in *Proc. ASME IMECE 2005*, 2005, IMECE05–81679.

[14] K. M. Lakin, "Modeling of thin film resonators and filters," in *Proc. IEEE MTT-S Int. Microwave Symp. Dig.*, Jun. 1992, pp. 149–152.

[15] G. Piazza, P. J. Stephanou, and A. P. Pisano, "Single-chip multiple-frequency AlN MEMS filters based on contour-mode piezoelectric resonators," *J. Microelectromech. Syst.*, vol. 16, no. 2, pp. 319–328, Apr. 2007.

[16] V. Kaajakari, T. Mattila, A. Lipsanen, and A. Oja, "Nonlinear mechanical effects in silicon longitudinal mode beam resonators," *Sens. Actuators A*, vol. 120, pp. 64–70, 2004.

Matteo Rinaldi (S'08) received his first level Laurea degree (B.Sc.) and second level Laurea degree (M.Sc.) in electronic engineering with honors from the University of Rome Tor Vergata, Rome, Italy, in 2004 and 2006, respectively.

He is currently working toward his Ph.D. degree in electrical and systems engineering at the University of Pennsylvania (UPenn), Philadelphia, PA. His research interests primarily include micro/nano electromechanical systems (MEMS/NEMS) devices, micro/nano AlN piezoelectric gravimetric sensors for multiple VOC detection, nano-sensitive layers for enhanced gas vapors adsorption, super high frequency (SHF) nanoelectromechanical resonators for RF and sensing applications.

He is a student member of IEEE; the IEEE Ultrasonics, Ferroelectrics, and Frequency Control Society, and the IEEE Electron Devices Society. Mr. Rinaldi was the recipient of the Best Student Paper Award at the 2009 IEEE European Frequency and Time Forum–International Frequency Control Symposium (EFTF-IFCS 2009) joint conference.

Chiara Zuniga (S'08) received her first level Laurea degree (B.S.), second level Laurea degree (M.Sc.) in electronic engineering with honors from the University of Rome Tor Vergata, Rome, Italy, and her M.S. in electrical engineering from the University of Pennsylvania (UPenn), Philadelphia, PA, in 2004, 2006, and 2009, respectively.

She is currently working toward her Ph.D. degree in electrical and systems engineering at the University of Pennsylvania. Her research interests primarily include micro/nano electromechanical systems (MEMS/NEMS) devices and sensor read-out circuits, in particular oriented towards the design of label-free biosensors integrated with micro/nanofluidic channels for real-time measurements.

She is a student member of IEEE and the IEEE Ultrasonics, Ferroelectrics, and Frequency Control Society.

Chengjie Zuo (S'07) received his B.S. degree in electronic information science and technology from the University of Science and Technology of China (USTC), Hefei, Anhui, China, in 2004 and his M.Sc. degree in electrical engineering with honors from the Delft University of Technology (TU Delft), Delft, The Netherlands, in 2006. He is currently working toward his Ph.D. degree in electrical and systems engineering at the University of Pennsylvania (UPenn), Philadelphia, PA. His research interests primarily include micro/nano electromechanical systems (MEMS/NEMS) devices, analog and RF integrated circuits (IC), and MEMS-IC integration and co-design. He is a student member of IEEE.

Gianluca Piazza (S'00–M'05) is a Wilf Family Term Assistant Professor in the department of Electrical and Systems Engineering (ESE) at the University of Pennsylvania. He received his Ph.D. degree from the University of California, Berkeley where he developed a new class of AlN contour-mode vibrating microstructures for RF communications. He has more than 10 years of experience working with piezoelectric materials and more than 40 referred publications in the area. He also holds two device patents in the field of micromechanical resonators. He received the IBM Young Faculty Award in 2006. His research interests focus on piezoelectric micro and nano electromechanical systems (MEMS/NEMS) for RF wireless communications, biochemical detection, wireless sensor platforms and all mechanical computing. He also has general interest in the areas of micro/nano fabrication techniques and integration of micro/nano devices with state-of-the-art electronics.